Archives of Mechanics • Archiwum Mechaniki Stosowanej • 31, 5, pp. 679–693, Warszawa 1979

Shock wave induced condensation in retrograde vapour

M. BRATOS (WARSZAWA) and G. E. A. MEIER (GÖTTINGEN)

THE PROCESS of shock wave induced condensation in retrograde fluids was investigated theoretically with the inclusion of a numerical example for C_8F_{16} (perfluorodimethylcyclohexane). For pure water steam and for moist air the phase transition is caused by the expansion of the gas, but in the case of retrograde gas, condensation can also take place as a result of compression. Compression in the retrograde vapour is performed by the incident shock wave travelling in a shock tube. Two principal effects of the condensation on the flow as a whole are: the transfer of a portion of the vapour phase to the liquid state and the heating of the remaining vapour. Heating is formed by the absorption of the condensation heat from the condensed phase. For retrograde fluids the effect of vapour removal dominates the heating. Because of this, the stream pressure and temperature in the constant area flow tend to decrease in the supersonic case and to rise in the subsonic case. This is just the opposite to the behaviour of a regular fluid. Numerical computations were done for different shock waves. Profiles for pressure, density, temperature increase and droplet formation in the condensation zone are calculated.

W pracy badano przepływ gazu typu retrograde z kondensacją. W przypadku przepływów pary wodnej lub wilgotnego powietrza przejście fazowe (para-ciecz) występuje na skutek ekspansji gazu. W gazach typu retrograde kondensacja może być spowodowana ich sprężaniem. W pracy rozpatrywano kondensację wywołaną w przepływie przez falę uderzeniową poruszającą się w rurze uderzeniowej. W przepływie występują dwa efekty związane z przemianą fazową. Mianowicie, kondensacja powoduje z jednej strony przejście części pary z fazy gazowej do ciekłej, a z drugiej ogrzanie pozostałej części pary. Dla gazów typu retrograde, w przeciwieństwie do gazów regularnych (np. para wodna, $p < 30$ bar – gaz regularny), efekt usuwania części pary z fazy gazowej do ciekłej dominuje nad efektem podgrzewania fazy gazowej. Dlatego też w przepływie gazu retrograde z kondensacją w rurze uderzeniowej ciśnienie i temperatura wzrastają w części poddźwiękowej przepływu (za falą uderzeniową). Obliczenia numeryczne przeprowadzono dla różnych modeli kondensacji i różnych fal uderzeniowych. Uzyskano strukturę strefy kondensacji za falą uderzeniową.

В работе исследовано течение газа типа ретрограде с конденсацией. В случае течений водяного пара или влажного воздуха фазовый переход (пар-жидкость) выступает вследствие расширения газа. В газах типа ретрограде конденсация может быть вызвана их сжатием. В работе рассматривается конденсация вызванная ударной волной движущейся в ударной трубке. В течении выступают два эффекта связанные с фазовым превращением. Именно, конденсация вызывает с одной стороны переход части пара из газовой фазы в жидкую, а с другой стороны нагрев остальной части пара. Для газов типа ретрограде, в противовес регулярным газам (например водяной пар, $0 < 30$ бар — регулярный газ), эффект удаления части пара из газовой фазы в жидкую преобладает над эффектом нагрева газовой фазы. Поэтому в течении газа типа ретрограде с конденсацией в ударной трубке, давление и температура возрастают в дозвуковой части течения (за ударной волной). Численные расчеты проведены для разных моделей конденсации и разных ударных волн. Получена структура зоны конденсации за ударной волной.

Notation

B second virial coefficient,
c_p, c_v specific heats (for non-ideal gas),
c_p^0, c_v^0 ideal-gas specific heats,
D self-diffusion coefficient,

h_{fg} specific heat of phase transition,
h_L specific liquid enthalpy,
h_m specific vapour-liquid mixture enthalpy,
h_v specific vapour enthalpy,
I^* nucleation rate,
k thermal conductivity,
k_B Boltzman constant,
m droplet mass,
$\tilde{m}$ mass of one vapour molecule,
$\mathcal{M}$ molecular weight,
M Mach number,
p vapour pressure,
p_c, T_c, V_c critical pressure, temperature and volume (per unit mass),
p_r, T_r, V_r reduced vapour pressure, temperature and volume:
$p_r = p/p_c,\ T_r = T/T_c,\ V_r = V/V_c$,
$p_\infty(T)$ flat-film saturation pressure corresponding to the temperature T,
$p_{\infty r} = p_\infty/p_c$ reduced saturation pressure over a flat film,
r droplet radius,
$\bar{r}$ „surface-averaged" droplet radius,
r^* critical radius,
$\mathcal{R}$ universal gas constant,
$R = \mathcal{R}/\mathcal{M}$,
S supersaturation,
T vapour temperature,
T_D droplet temperature,
t time,
u flow speed,
V specific vapour volume,
V_{mc} volume of one vapour molecule,
w acentric factor,
x coordinate in flow direction,
α_c Riedel parameter,
γ ratio of specific heats,
η dynamic viscosity,
μ condensate mass fraction,
ϱ vapour density (at the infinity from the droplet),
ϱ_D vapour density at the droplet surface,
ϱ_m vapour-liquid mixture density,
σ surface tension,
τ_d delay time,
$p_1, T_1, M_1, V_1, \varrho_1$ parameters in front of the shock wave,
$p_2, T_2, M_2, V_2, \varrho_2$ parameters behind the shock wave.

Subscripts

c critical parameters,
D droplet,
L liquid,
m mixture,
r for a droplet with radius r (also for reduced parameters),
v vapour,
∞ flat interface.

Superscript

$*$ indicates critical droplet size.

1. Introduction

RECENTLY, a number of works both theoretical and experimental have been devoted to so-called retrograde fluid. In this work the condensation induced by the shock wave in retrograde fluid — perfluorodimethylcyclohexane (C_8F_{16}) is investigated.

For regular fluids (such as water) the adiabatic expansion leads to condensation. In the case of retrograde fluids, such as octane or perfluorodimethylcyclohexane, the adiabatic compression leads to condensation. It is illustrated in Fig. 1.

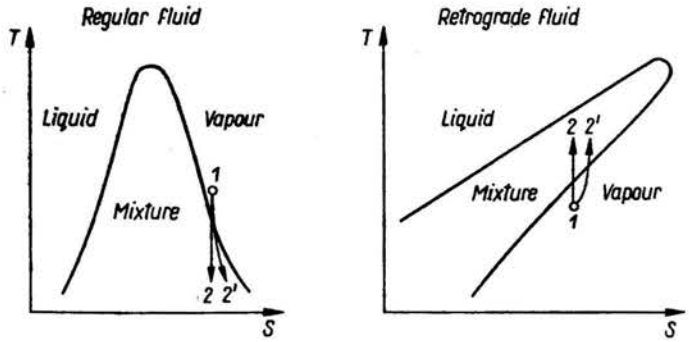

FIG. 1. Temperature-entropy diagram. Adiabatic condensation of regular and retrograde fluids. ($1 \to 2$, isentropic condensation, $1 \to 2'$, nonisentropic condensation).

There is a large class of such fluids; for example, all fluids in paraffin hydrocarbon series above the complexity level of propane are retrograde. G. E. A. MEIER, P. THOMPSON [1, 2] investigated experimentally the complete condensation shock waves in retrograde fluids using a shock tube.

The complete condensation shock waves were produced by shock waves reflected from the rigid end-wall of the tube. Pressure was measured behind the incident and the reflected shock waves.

In the present work we intend to describe the droplet-condensation zone behind the incident shock wave in a retrograde fluid such as perfluorodimethylcyclohexane. In addition to that, the influence of the condensation on the profiles of different quantities of state will be shown.

2. The physical model assumptions. Governing equations

The flow is treated as one-dimensional, the influence of walls being neglected. The effect of conductivity of the vapour is taken into account only in the vicinity of the macroscopic droplets. The vapour phase behaves like an ideal gas, that is, it obeys the thermal equation for the ideal gas and the internal energy and the enthalpy are functions of temperatures only.

The liquid phase is assumed to be incompressible. It is present in the form of spherical droplets which do not interact with each other; hence the coagulation effects are neglected.

The droplets have the same velocity as vapour and the temperature at the surface of the droplet is the same as inside.

The droplets appear just behind the shock wave in the process of the spontaneous, homogeneous nucleation. The homogeneous nucleation is described by the Frenkel-Zeldovich steady-state nucleation model. Therefore the nucleation rate is described in the following form [3–7]:

$$I^* = \left(\frac{p}{k_B T}\right) V_{mc} \sqrt{\frac{2\sigma}{\pi \tilde{m}}} \exp\left(-\frac{4\pi\sigma r^{*2}}{3k_B T}\right), \tag{2.1}$$

where

$$r^* = \frac{2\sigma}{\varrho_L R T \ln(p/p_\infty)}, \quad R = \frac{\mathscr{R}}{\mathscr{M}}. \tag{2.2}$$

The nucleation rate depends strongly on the supersaturation and on the surface tension.

As regards surface tension, for the retrograde liquid the bulk value of the surface tension σ_∞ depends on the temperature as follows:

$$\sigma_\infty(T) = \sigma_\infty(T_0) \left[\frac{\left(1-\frac{T}{T_c}\right)}{\left(1-\frac{T_0}{T_c}\right)}\right]^{1.2}. \tag{2.3}$$

This is the GAMBILL [8, 9] formula.

The exponent 1.2 is strictly applicable to nonpolar gases; T_c is the critical temperature.

The critical temperature of a pure material may be defined as the maximum temperature at which liquid and vapour phases can coexist in equilibrium; above this temperature no liquid phase is then possible.

The vapour pressure at this temperature is termed the critical pressure (p_c) and the volume per unit mass, the critical volume (V_c).

From a mathematical sense the definition of the critical point is

$$\left(\frac{dp}{dV}\right)_{T_c} = \left(\frac{d^2p}{dV^2}\right)_{T_c} = 0. \tag{2.4}$$

If for a certain temperature the value of the interfacial tension (for the flat surface between two phases) is known, then formula (2.3) makes it possible to get the values of surface tension for any other temperatures.

The influence of the radius on the droplet surface tension is given by the TOLMAN [7, 10, 11] relation:

$$\sigma_r = \sigma_\infty \left(1 - \frac{2}{\tilde{k}r} + \frac{2}{\tilde{k}^2 r^2}\right), \tag{2.5}$$

where $1/\tilde{k} \approx (2 \div 5) \cdot 10^{-8}$ cm.

Tolman suggests that the surface tension for a droplet lies below its bulk value. We also admit this correction.

It should be noted that for the determination of the critical radius r^* and nucleation rate, the value of supersaturation $S = p/p_\infty$ is required, where p_∞ is the equilibrium pressure of a vapour coexisting with its liquid phase.

The equilibrium pressure is given by the Clausius-Clapeyron equation for retrograde fluids [8, 12–14]. It is the so-called Riedel equation for retrograde fluids:

$$p_{\infty r} = f(T_r, \alpha_c),$$

as follows:

$$\begin{aligned} \log p_{\infty r} &= -\Phi(T_r) - (\alpha_c - 7)\Psi(T_r), \\ \Phi(T_r) &= 0.118\varphi(T_r) - 7\log T_r, \\ \Psi(T_r) &= 0.0364\varphi(T_r) - \log T_r, \\ \varphi(T_r) &= 36/T_r + 42\ln T_r - 35 - T_r^6, \end{aligned} \tag{2.6}$$

where $T_r = T/T_c$ and $p_r = p/p_c$ and where $p_{\infty r} = 1$ when $T_r = 1$. α_c is the so-called Riedel parameter [8, 14] which could be estimated from the properties of normal boiling point and critical ones.

We use it in the form of the THOMPSON [1] correlation formula:

$$\alpha_c = 5.7 + 0.34\left(\tilde{c}_v - \frac{3}{2}\right)^{1/2}, \quad \text{where} \quad \tilde{c}_v = c_v/R, \tag{2.7}$$

where c_v is the specific heat.

Just behind the shock wave the size of the droplet is very small, less than the mean molecular free path in the gas. Therefore the Hertz-Knudsen model for the mass and energy exchange between two phases is applicable here [15].

Due to the condensation, the droplets grow up and at a certain distance from the shock wave they become larger than the mean molecular free path.

At this stage we may use the following equations [16]:

$$\frac{dm}{dt} = 4\pi r D(\varrho - \varrho_D), \quad \text{where} \quad r = \bar{r}. \tag{2.8}$$

This describes the flux of vapour mass towards the droplet in the form of Fick's law of diffusion for a spherical droplet.

To describe the energy exchange between two phases the equation for conduction of heat away from the droplet surface may be written in the form of the Fourier equation:

$$h_{fg}\frac{dm}{dt} = h_{fg} \cdot 4\pi r^2 \varrho_L \frac{dr}{dt} = -4\pi k r(T_D - T), \tag{2.9}$$

where

$$r = \bar{r} \quad \text{and} \quad \frac{dr}{dt} = \frac{d\bar{r}}{dt}.$$

These two equations are needed to compute the droplet temperature T_D and then the rate of droplet growth dr/dt. Here T is the temperature of the vapour at a certain distance from the droplet (temperature of a vapour environment).

There is a number of physical quantities entering these equations.

First: h_{fg} is the specific heat of phase transition, k is the thermal conductivity of the retrograde vapour.

For the estimation of the thermal conductivity coefficient we use the semi-empirical Eucken correlation. This correlation was introduced for polyatomic gases at low pressures [8].

We must also have the value of a dynamic viscosity η and to this end the BROMLEY and WILKE [17] empirical formula is applied.

This formula is an empirical correlation of the viscosity values obtained in the Chapman-Enskog theory with the critical properties [8, 18–19]:

$$\eta = \frac{0.00333 \cdot (\mathcal{M}T_c)^{1/2} f_1(1.33T_r)}{V_c^{2/3}}. \tag{2.10}$$

The self-diffusion coefficient values are also taken from the semi-empirical formula obtained in the Chapman-Enskog theory [8, 19–21]:

$$D = 1.2(\mathcal{R}T/\mathcal{M}P)\,(1.1)\eta, \tag{2.11}$$

where $\mathcal{R}$ — universal gas constant, T, P — vapour temperature and pressure, $\mathcal{M}$ — mole mass, and where η is expressed in poises, P in atmospheres, D in square centimeters per second.

ϱ_D is the vapour density at the droplet surface and

$$\varrho_D = p_D/RT_D, \tag{2.12}$$

p_D is the ambient pressure which would be necessary to keep the droplet in equilibrium, both droplet and vapour having the temperature T_D. Using the Helmholtz equation this pressure is

$$p_D = p_\infty(T_D)\exp\{2\sigma/\varrho_L RT_D r\}, \tag{2.13}$$

where r is the droplet radius and $p_\infty(T_D)$ is the flat-film saturation pressure corresponding to the temperature T_D.

In each cross-section of the shock tube the radii of all droplets are the same and equal to the so-called "surface-averaged" droplet radius [15, 22].

In our previous work [23] it was shown that a more realistic model with the radii distribution function of droplets gives almost the same results (in one-dimensional flow) as a model of a "surface-averaged" droplet radius adopted from HILL [22].

We also assume that a behaviour of this artificial droplet with a "surface-averaged" droplet radius is the same as the physical one and its growth is described by Fick's law of diffusion and the Fourier equation for conduction.

It is obvious to take as the initial condition for the droplet radii its critical value: $r_0 = \bar{r} = r^* \rightarrow$ and it implies that its temperature must be equal to the gas temperature

$$T_D = T.$$

One-dimensional, two-phase flow is described by the mass, momentum and energy conservation equations for a vapour-liquid mixture:

$$\frac{1}{\varrho_m}\frac{d\varrho_m}{dx} + \frac{1}{u}\frac{du}{dx} = 0, \tag{2.14}$$

$$\frac{dp}{dx} + \varrho_m u \frac{du}{dx} = 0, \tag{2.15}$$

$$\frac{d}{dx}\left(h_m + \frac{u^2}{2}\right) = 0, \tag{2.16}$$

where

$$\varrho_m = \frac{\varrho \varrho_L}{(1-\mu)\varrho_L + \mu\varrho} \tag{2.17}$$

and

$$h_m = (1-\mu)h_v + \mu h_L. \tag{2.18}$$

To complete the system of equations the thermal and calorical equations of state are required.

In the considered condensation model the relative rate of formation of a new phase is given by one integrodifferential equation:

$$u\frac{d\mu}{dx} = \left(\frac{\varrho_L}{\varrho_m}\right)\left[\frac{4}{3}\pi r_0^3 I^*(x) + \left\{\int_0^x 4\pi\left(r_0 + \int_{x_1}^x \frac{dr}{dt}\frac{dx_2}{u}\right)^2 \frac{I^*(x_1)}{\varrho_m(x_1)}\frac{dx_1}{u}\right\}\varrho_m \frac{dr}{dt}\right]. \tag{2.19}$$

The first term on the right-hand side is the condensation rate due to the formation of new droplets in a fluid element at x. The second term describes the condensation rate due to the growth of all droplets which have been created somewhere before a fluid element at x along the streamline.

3. Results and conclusions

The calculations were performed for different conditions in front of the shock wave, namely for different Mach numbers, temperature and density.

The typical behaviour of parameters' distributions in the condensation zone for retrograde fluids is illustrated in Fig. 2.

Attention should be paid to the fact that, in retrograde fluid, condensation causes the increase of both temperature and pressure in the subsonic flow. One can compare the condensation process in the regular fluid, for example water vapour(1), to the heat addition. When condensation takes place either in regular or retrograde fluid, it causes a removal of a part of the vapour phase (because of phase transition) and the increase of temperature of vapour due to the energy released in the process of condensation.

In the case of regular fluid heating has a larger effect on the stream properties than the vapour removal, whereas for retrograde fluid the effect of a removal of the part of the vapour seems to be dominant. As a result of this, we observe the rise of pressure and temperature in the subsonic flow.

The condensation zone structure depends strongly on the assumptions connected with the surface tension. Figure 3 illustrates this fact.

As an example we can see the results for the case where there is no correction of the interfacial tension σ with respect of the droplet size.

The deviation between the values of a new phase mass fraction obtained in both models (with and without the Tolman correction of the droplet surface tension) is about 50%.

(1) Water vapour behaves like a „regular fluid" for the pressure $p < 30$ bar [24].

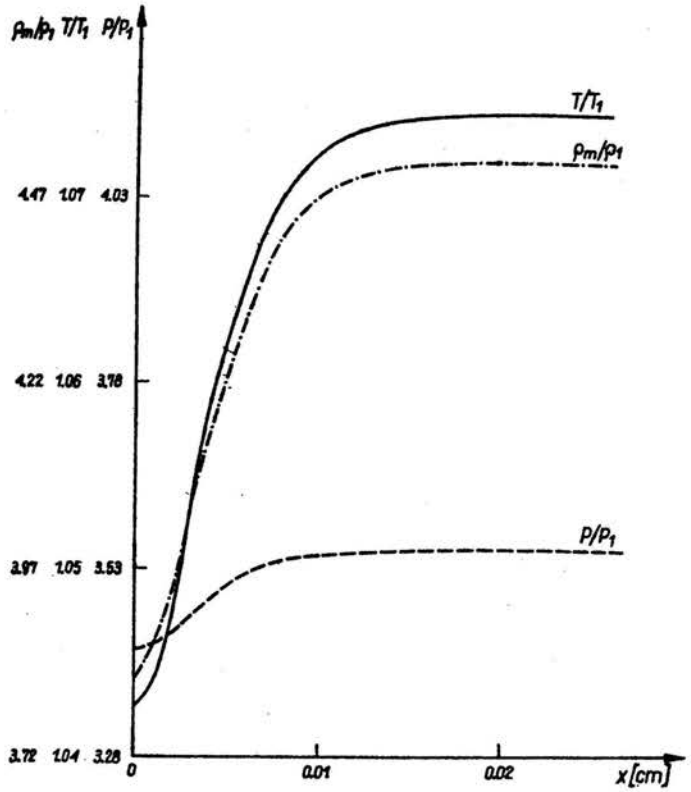

FIG. 2. Profiles of different quantities of state in the condensation zone behind the shock wave ($V_1 = 79$ cm³/g, $T_1 = 393$°K, $M_1 = 1.91$).

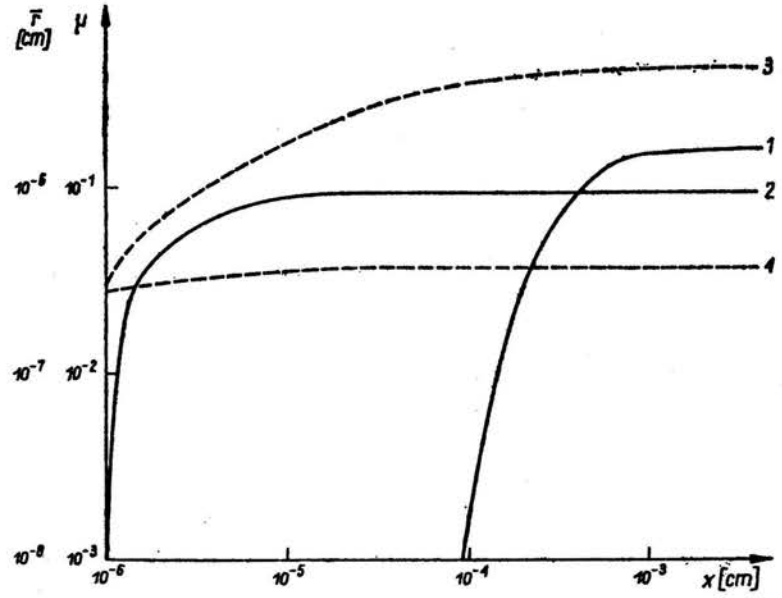

FIG. 3. The distributions of the „surface-averaged" radius and the condensate mass fraction in the condensation zone (curves: *1, 3* — without the Tolman correction, curves *2, 4* — with the Tolman correction; curves 1,2 — $\mu(x)$, curves 3,4 — $\bar{r}(x)$). Parameters in the front of a shock wave: $V_1 = 79$ cm³/g, $T_1 = 403$°K, $M_1 = 2.16$.

The final size of droplets in the case where the Tolman correction was neglected is of one order greater and the change of the length of the condensation zone is even greater — almost two orders of magnitude.

One can ask whether the assumption of the ideal gas is not too restrictive. To answer this question we repeated all calculations taking into account the assumptions of gas non-ideality.

The effect of the intermolecular forces was here taken into account by the approximation to the second virial coefficient.

Therefore the thermal equation of state is

$$p = \varrho RT[1+\varrho B(T)] \tag{3.1}$$

and the caloric equation of state is as follows:

$$h = h(p, T) = h_1 + c_p^0(T-T_1) - \frac{A(T_1)}{2B(T_1)}[RT_1 - \sqrt{R^2T_1^2+4p_1RT_1B}] - \frac{A(T)}{2B(T)}[\sqrt{R^2T^2+4pRTB}-RT], \tag{3.2}$$

where enthalpy is the function of pressure and temperature and where

$$A = \left(\frac{\partial B}{\partial T}\right)_p T - B, \tag{3.3}$$

h_1 — the specific enthalpy for the vapour state characterized by the pressure and the temperature p_1, T_1.

Using the PITZER, CURL model [8, 25–27] we could find a value of the second virial coefficient B.

Here the second virial coefficient is a function of temperature, critical properties and the so-called acentric factor w, which characterizes the acentricity of non-spherical molecules:

$$B = B^0 + wB^1, \tag{3.4}$$

$$B^0 = f^0(T, T_c, p_c) = \frac{RT_c}{p_c}[0.1445 - 0.330/T_r - 0.1385/T_r^2 - 0.0121/T_r^3], \tag{3.5}$$

$$B^1 = f^1(T, T_c, p_c) = \frac{RT_c}{p_c}[0.073 + 0.46/T_r - 0.50/T_r^2 - 0.097/T_r^3 - 0.0073/T_r^8], \tag{3.6}$$

$$w \equiv -1.0 - \log p_{\omega r} \quad \text{at} \quad T_r = 0.7. \tag{3.7}$$

For the perfluorodimethylcyclohexane (C_8F_{16}) the acentric factor was estimated as equal to $w = 0.4535$.

Figure 4 shows the change due to the non-ideality of the gas on Hugoniot's curve.

The non-dimensional pressure distributions and mass fraction distributions for the new phase for both ideal and non-ideal gases are shown in Fig. 5. As we can see in this figure, the relative changes are not very great for pressure and mass concentration of a new phase.

However, the size of droplets differs considerably (Fig. 6) — one order of magnitude.

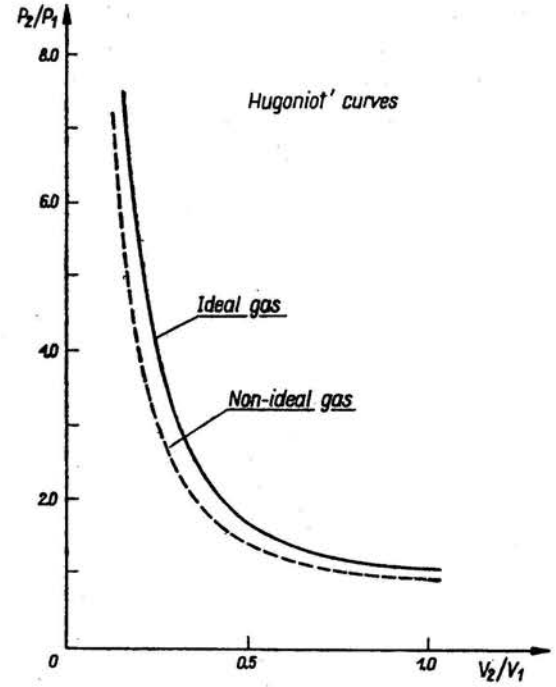

FIG. 4. Hugoniot's curves for ideal and non-ideal gases.

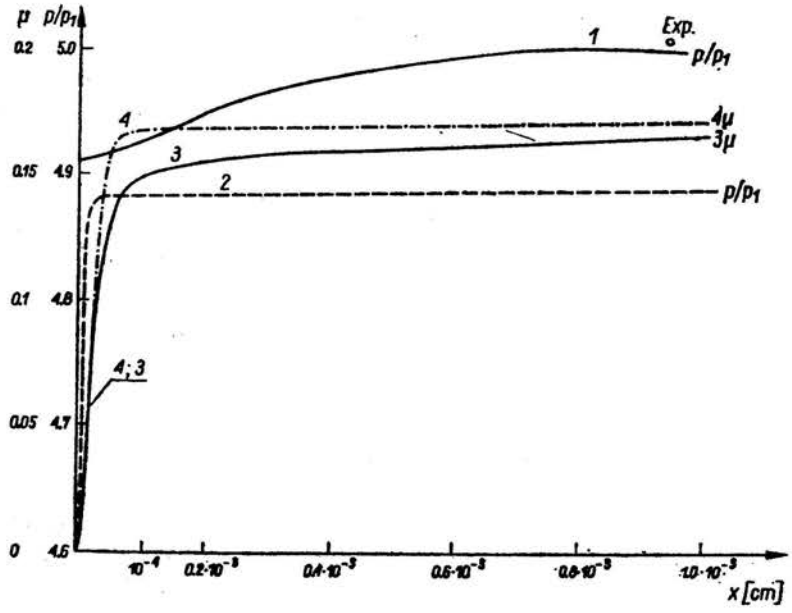

FIG. 5. The distribution of the condensate mass fraction and the nondimensional pressure in the condensation zone for ideal and non-ideal gases. Parameters in the front of a shock wave: $V_1 = 79$ cm^3/g, $T_1 = 403$°K, $M_1 = 2.16$. (Curves *1, 3* — non-ideal gas, curves *2, 4* — ideal gas).

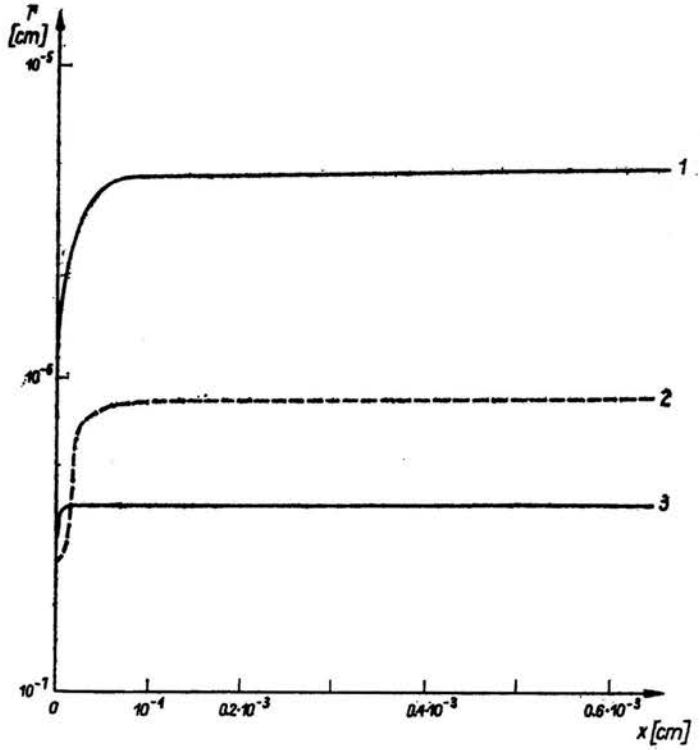

FIG. 6. The „surface-averaged" radius distributions behind shock wave (in the condensation zone) for different models of phase transition (curves *1, 3* — non-ideal gas, curve *2* — ideal gas, curves *1, 2*: $\sigma = F(\sigma_\infty, T, T_c)$, curve *3*: $\sigma = F_1(\sigma_\infty, T, T_c, \bar{r})$). $V_1 = 79$ cm³/g, $T_1 = 403$°K, $M_1 = 2.16$.

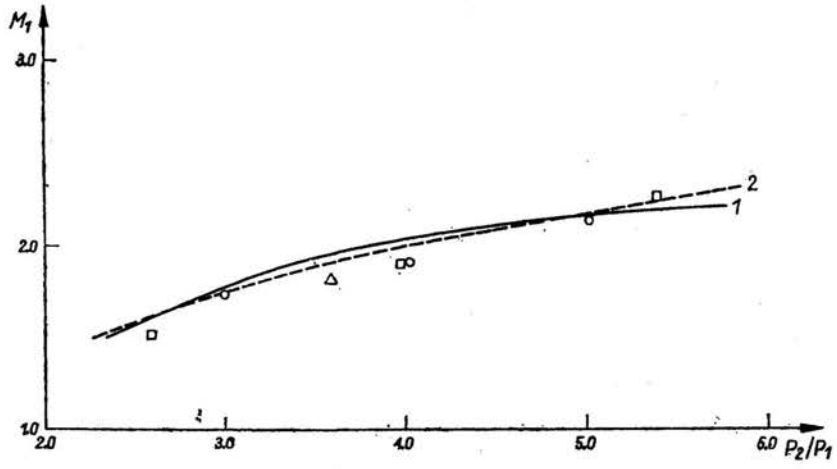

Fig. 7. The comparison between the theory and the experiment. M_1 versus p_2/p_1. Curves *1, 2*—(theory): *1* — non-ideal gas, *2* — ideal gas ($V_1 = 79$ cm³/g, $T_1 = 403$°K).
Experiment: □ $V_1 = 161$ cm³/g, △ $V_1 = 159$ cm³/g, ○ $V_1 = 79$ cm³/g.

In the case of a non-ideal gas, the relaxation zone is also one order of magnitude longer than in the case of ideal gas.

In the experiments(2) the pressure behind the relaxation zone in the two-phase equilibrium zone was measured.

As we can see in Fig. 7 (p_2/p_1 versus M_1), both theoretical results for ideal and non-ideal gases give good agreement with these experimental data.

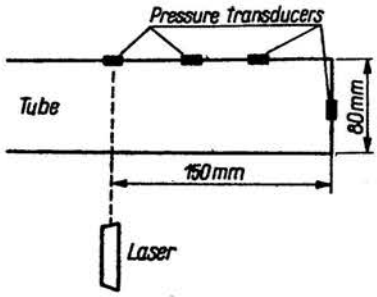

FIG. 8. Position of pressure transducers and a laser beam in the test section of the shock tube.

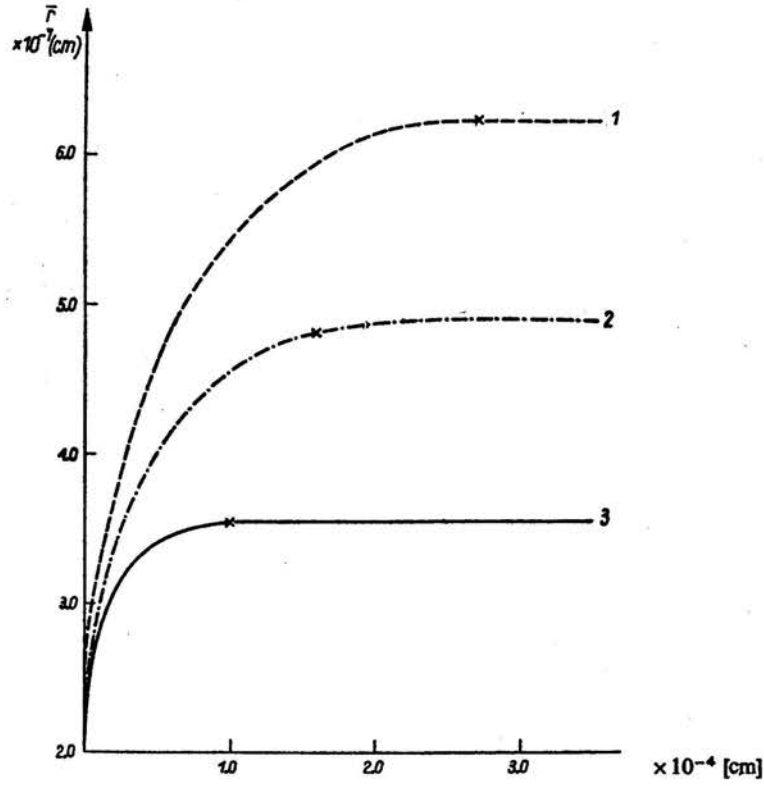

FIG. 9. The distributions of the „surface-averaged" radius in the condensation zone for the different shock waves ($V_1 = 80.01$ cm^3/g, $T_1 = 403$°K and $M_1 = 2.1$ — curve *1*, $M_1 = 2.15$ — curve *2*, $M_2 = 2.25$ — curve *3*). The star * indicates the observable influence of condensation on the laser beam.

(2) The measurements were performed by H. D. Speckmann from Max Planck Institut für Strömungsforschung, Göttingen.

To find out which approach should be used (in this range of pressures), much more refined measurements are needed such as the measurement of the mass concentration of a liquid phase (or the droplet concentration) and the measurement of final droplet sizes.

The Rayleigh scattering of laser light was used as a diagnostic means to determine the location of such a condensation region, at which the concentration and the sizes of the droplets are sufficiently large so that the droplets can be detected. The wave length of the laser light used in the experiment was 632.8 nm and the beam diameter 0.9 mm. The "delay time" τ_d, which characterizes the condensation rate in the flow, was de-

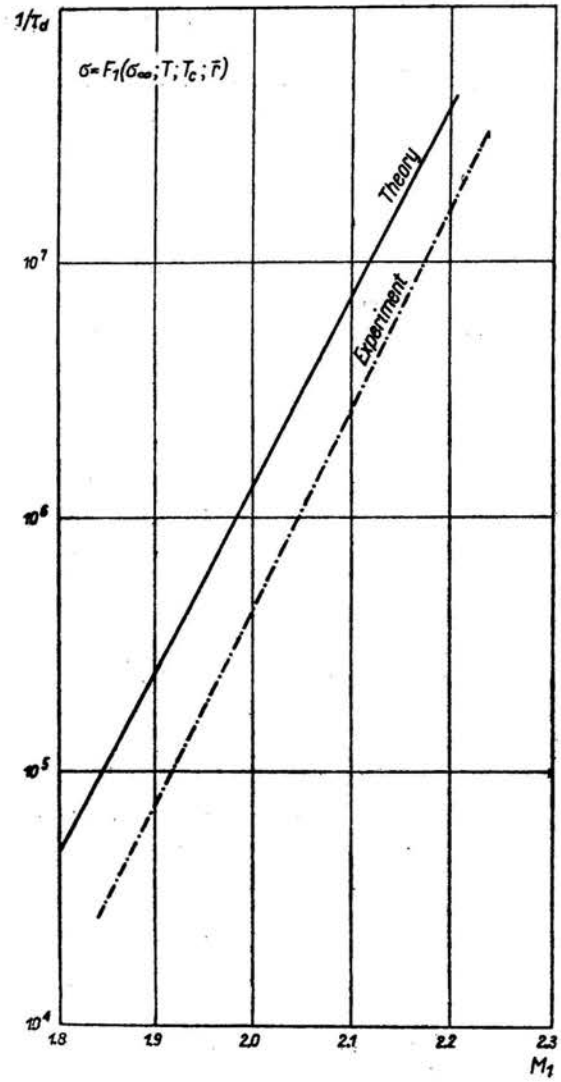

FIG. 10. The comparison between the theory (non-ideal gas model, Tolman correction) and the experiment. $1/\tau_d$ versus M_1.

termined experimentally. τ_d was defined as the difference between two instants of time: at which the shock wave passed through the laser beam (it was recorded by the pressure transducer) and at which laser light attenuation began (Fig. 8).

The onset of the observable (i.e. experimentally detectable by the laser light beam) condensation in the flow is marked in Fig. 9 by the star.

Taking into account the numerical values of the droplet sizes and the droplet concentration, we could calculate [28, 29] the relative attenuation of the intensity of the laser light and then the theoretical "delay time" τ_d.

Figure 10 shows the comparison of the experimental "delay time" τ_d with the theoretical one for the different Mach numbers in front of the shock wave. The theoretical results were obtained using a non-ideal gas model and the Tolman correction. The good agreement between the theory and the experiment indicates that the Tolman correction is necessary in the right description of the nucleation and the droplet growth for retrograde fluids.

References

1. P. A. THOMPSON, D. A. SULLIVAN, *On the possibility of complete condensation shock waves in retrograde fluids*, J. Fluid Mech., **70**, 4, 639–649, 1975.
2. G. DETTLEFF, P. A. THOMPSON, G. E. A. MEIER, *Initial experimental results for liquefaction shock waves in organic fluids*, Arch. Mech., **28**, 5–6, 827–836, 1976.
3. P. P. WEGENER (ed.), *Nonequilibrium flows*, M. Dekker, New York and London 1969.
4. J. P. HIRTH, G. M. POUND, *Condensations and evaporation. Nucleation and growth kinetics* (Progress in Material Science), **11** (ed. B. Chalmers), Pergamon Press, London 1963.
5. A. C. ZETTLEMOYER (ed.), *Nucleation*, M. Dekker Inc., New York 1969.
6. M. VOLMER, *Kinetik der Phasenbildung*, Steinkopff, Dresden und Leipzig 1939.
7. G. A. SALTANOV, *Sverzvukovye dvukhfaznye tečeniya*, Izd. Vyšeišaja škola, Minsk 1972.
8. R. C. REID, T. K. SHERWOOD, *The properties of gases and liquids*, McGraw-Hill Book Comp., New York 1958, 1966.
9. W. R. GAMBILL, Chem. Engng., **64**, 5, 143, 1958.
10. R. C. TOLMAN, *Effects of droplet size on surface tension*, J. Chem. Phys., **17**, 1949.
11. A. G. AMELIN, *Teoretičeskie osnovy obrazovanija tumana pri kondensatii para*, Izd. Khimija, Moskwa 1972.
12. R. PLANK, L. RIEDEL, Ing.-Arch., **16**, p. 255, 1948.
13. R. PLANK, L. RIEDEL, Texas J. Sci., **1**, 86, 1949.
14. L. RIEDEL, Chem.-Ing.-Tech., **26**, p. 83, 1954.
15. M. BRATOS, M. JAESCHKE, *Two-dimensional flows with non-equilibrium phase transitions*, IFTR Report, Warsaw 1974.
16. B. J. MASON, *The physics of clouds*, Oxford Univ. Press, London 1957.
17. L. A. BROMLEY, C. R. WILKE, Ind. Engng. Chem., **41**, p. 1641, 1951.
18. S. CHAPMAN, T. G. COWLING, *The mathematical theory of non-uniform gases*, Cambridge Univ. Press, New York 1939.
19. J. O. HIRSCHFELDER, Ch. F. CURTISS, R. B. BIRD, *Molecular theory of gases and liquids*, Univ. Wisconsin Naval Research Laboratory 1954 or J. Wiley and Sons Inc., New York 1954.
20. S. WEISSMAN, E. A. MASON, J. Chem. Phys., **37**, p. 1289, 1962.
21. S. WEISSMAN, J. Chem. Phys., **40**, p. 3397, 1964.
22. P. G. HILL, *Condensation of water vapour during supersonic expansion in nozzles*, J. Fluid Mech., **25**, p. 593, 1966.

23. M. BRATOS, G. E. A. MEIER, *Two-dimensional, two-phase flows in a Laval nozzle with non-equilibrium phase transition*, Arch. Mech., **28**, 5–6, 1025–1037, 1976.
24. R. PUZYREWSKI, W. STUDZIŃSKI, *Real gas effects on condensation process in water vapour flow*, XIII Symp. on Advanced Problems and Methods in Fluid Mechanics, Olsztyn 1977.
25. K. S. PITZER, J. Am. Chem. Soc., **77**, p. 3427, 1955.
26. K. S. PITZER, R. F. CURL, J. Am. Chem. Soc., **79**, p. 2369, 1957.
27. K. S. PITZER, R. F. CURL, *The thermodynamic properties of normal fluids*, Conf. on Thermodynamics and Transport Properties of Fluids, London, July 1957.
28. R. PUZYREWSKI, *Kondensacja pary wodnej w dyszy de Lavala*, PWN, Warszawa 1969.
29. H. C. VAN DE HULST, *Light scattering by small particles*, New York, J. Wiley and Sons Inc., London, Chapman and Hall Ltd. 1957.

POLISH ACADEMY OF SCIENCES
INSTITUTE OF FUNDAMENTAL TECHNOLOGICAL RESEARCH

and

MAX-PLANCK-INSTITUT FÜR STRÖMUNGSFORSCHUNG, GÖTTINGEN, FRG.

Received June 5, 1978.